AIMS Materials Science, 8(1): 42–61.
DOI: 10.3934/matersci.2021004
Received: 01 December 2020
Accepted: 28 January 2021
Published: 04 February 2021

http://www.aimspress.com/journal/Materials

Research article

Computation of shear strength equation for shear deformation of reinforced concrete deep beams using finite element method

G. Sri Harsha[1,*], P. Poluraju[2] and Veerendrakumar C. Khed[1]

[1] Department of Civil Engineering, Koneru Lakshmaiah Education Foundation, Vaddeswaram, AP, India
[2] Department of Civil Engineering, VR Siddhartha Engineering College, Vijayawada, AP, India

* **Correspondence:** Email: harsha.g3@kluniversity.in, Tel: +918331813053.

Abstract: This paper gives the analytical investigation of six reinforced concrete deep beams reinforced with horizontal and vertical web reinforcement. Reinforced concrete deep beams analysis is a complex problem where there is no exact solution. The effect of reinforcement distribution has been studied and compared to experimental investigation and various codes such as ACI 318 and IS 456. A new formula is proposed to define shear strength of deep beams. The codal equations are too traditional for predicting the shear strength of RC deep beams, so an improved and simplified equation was proposed using nonlinear finite element method by ABAQUS. The FE results are compared with experimental results in terms of ultimate loads, displacements, tension stress damage. The proposed shear strength equation predicts 80% of the experimental data in the range of 66–110% of measured shear strength. FE model results accurately predicted. The stress contours suggested high stresses in the path of cracks and low stresses in the uncracked regions.

Keywords: deep beams; shear strength prediction; damage tension; web reinforcement; shear span

1. Introduction

Structural members are categorized into two regions. The first one is Bernoulli region in which strain distribution for the entire section is linear. The second one is distributed region where the strain is nonlinear which appears to be in deep beams. Reinforced concrete deep beams have a wide variety of applications in structural engineering aspects like in the construction of wall footings, transfer girders, pier foundations, foundation pile caps. Also, the utilization of deep beams in high

rise structures for various commercial purposes is increased rapidly due to their ease of convenience and economical efficiency [1]. In olden days, deep beams are designed in a traditional way of experience or empirical formulae [2]. Now a days, the strut and tie method is using for design of deep beams according to various codes. The shear strength estimated by using ACI Code and EURO Code were overestimated than the predicted actual strengths calculated from Zsutty and Russo models [3]. Compressive strength of concrete at the initial days was very low and increases with increase in the age up to 28 days [4,5]. Failure occurs in deep beams with formation of cracks from the stress zone and thereby spreading to pressure zone [6]. The width of deep beam is not important on shear conduct for a/d proportions and diagonal crack dominates the flexure cracks at the initial stage of loading [7].

Use of Inclined shear reinforcement is not popular due to fabrication difficulty however despite diagonal cracking pattern of shear failure in deep beams, inclined position is effective compared to vertical position [8]. Minimum shear reinforcement must be provided according to the code to resist the shear cracks in deep beams. 0.2% is the appropriate shear reinforcement decided in theoretical analysis [9]. However, the final failure in deep beams occurs due to ultimate deflection with crushing of compression concrete [10]. The increase in web reinforcement increases the loading capacity of deep beams [11].

The finite element method gives a specific and realistic solutions to determine the nonlinear behavior of reinforced concrete deep beams. So, ABAQUS [12] software was used to predict the behavior of deep beams under 3-point bending configuration. The modeling technique was verified by validating the model prediction with the experimental work. Later, the results were compared with ACI-318-08 [13] recommendations. With the increase in load, the finite element analysis gives good results in the strain distribution of longitudinal reinforcement [14]. It also gives same crack patterns and load displacement response compared to experimental results. The method of introducing strut is more effective with the angle of inclination of more than 30° [15].

2. Research significance

Different codes of practice and several researchers propose different shear strength expressions for RC deep beams, a research gap still exists to minimize the strength ratio $\left(\frac{V_n^{TEST}}{V_n^{PRE}}\right)$ as scattering near the safety line $\left(\frac{V_n^{TEST}}{V_n^{PRE}} = 1.0\right)$ and to reduce the number of overestimated beams. In order to fill the gap, a refined shear strength equation is proposed by incorporating effect of web reinforcement, beam size, shear span-to-depth ratio and limitations of compressive strength of concrete on shear strength. The accuracy of prediction by the proposed equation is compared with finite element results and the experimental results. Further, two discrepancies of STM such as over conservativeness and negligence of effect of web reinforcement are refined in the proposed equation.

3. Modal geometry

3.1. Test data

All the specimens were tested under three-point bending with simply supported condition under the loading frame of capacity 2000 kN. Surface strain gauges were used to calculate the strains and linear variable displacement transducer was used to monitor deflections. Crack width is measured by using micrometer with an accuracy of 0.01 mm. Table 1 shows the percentage of horizontal and vertical shear reinforcement. Keeping the compressive strength constant, horizontal reinforcement is varied from 0.45% to 0.55% and vertical shear reinforcement is taken as 0.4% and 0.6%.

Table 1. Cross section and percentage of horizontal and vertical shear reinforcement of deep beams.

S. No	Beam ID	L (mm)	B (mm)	D (mm)	l/d	a/d	ρh%	ρv%
1	1D500	900	150	500	1.8	0.9	0.45	0.4
2	2D500	900	150	500	1.8	0.9	0.5	
3	3D500	900	150	500	1.8	0.9	0.55	
4	4D500	900	150	500	1.8	0.9	0.45	0.6
5	5D500	900	150	500	1.8	0.9	0.5	
6	6D500	900	150	500	1.8	0.9	0.55	

The experimental study consists of 6 deep beams of 150 mm width and 500 mm depth for a span of 900 mm with varying percentages of horizontal and shear reinforcement. The first three beams have been flexurally reinforced with three 16 mm diameter bars of HYSD 500 in a single layer and the tension region depth is 90 mm. The last three beams have been flexurally reinforced with four 16 mm diameter bars of HYSD 500 in double layer. Figure 1 shows the reinforcement details of all six deep beam specimens.

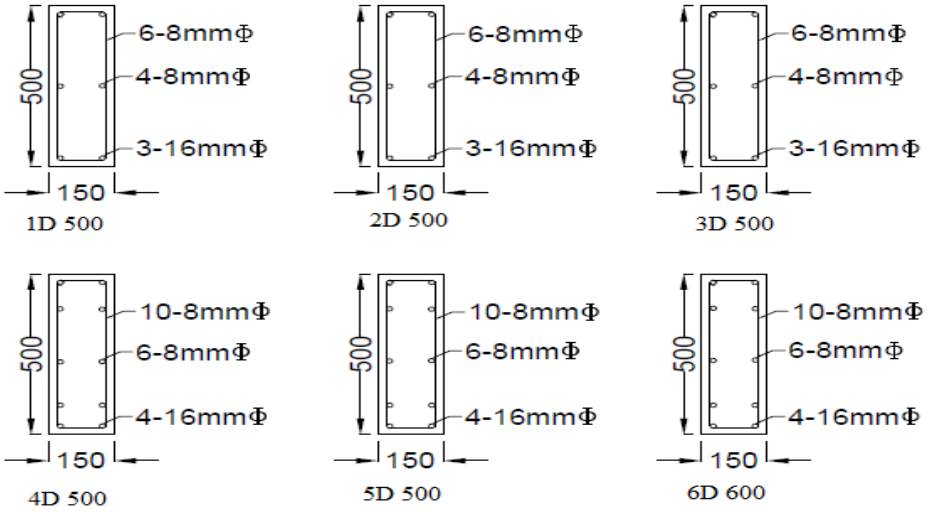

Figure 1. Cross-section details of deep beam specimens.

3.2. Test setup

Table 2 shows the values of compressive strength of concrete. All the specimens were cast using M 35 grade concrete to attain a target strength of 43.25 N/mm^2. The water–cement ratio is considered as 0.45 confirming to IS 10262-2009. The quantity of cement content and fine aggregate content obtained is 350.51 and 651.47 kg/m^3. A mixture of 10 and 20 mm coarse aggregates have been used for smooth finishing of specimens and quantity obtained for three sample cubes is 498.3 and 747.45 kg/m^3. 16 mm diameter high yield strength deformed bars of grade Fe 500 were used for flexural reinforcement and 8 and 12 mm diameter bars of grade Fe 500 were used for shear reinforcement (both horizontal and vertical). Table 3 determines the yield strength and ultimate strength of bars used for the experimental work. Figure 2 represents the arrangement of deep beam under the loading frame to measure ultimate load and deflection.

Table 2. Average compressive strength of concrete.

S. No	Age of specimen	Group-I mix load (kN)	Group-II mix load (kN)	Group-III mix load (kN)	Group-IV mix load (kN)
1	7 days	870	860	880	920
2	14 days	890	900	910	940
3	28 days	930	920	930	1040
Compressive strength (N/mm^2)		39.90	39.71	40.29	42.96

Table 3. Mechanical properties of steel reinforcement.

S. No	Bar diameter (mm)	Area (mm^2)	Yield strength (MPa)	Ultimate strength (MPa)
1	8	50.24	540.45	631.3
2	12	113.1	569.8	637.1
3	16	201	564.3	652.8

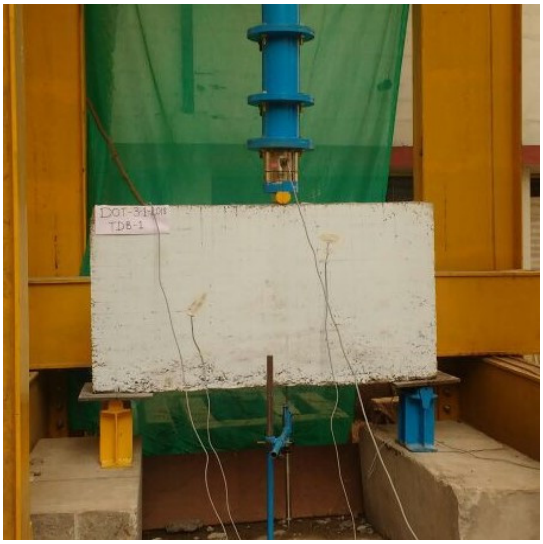

Figure 2. Loading frame setup.

4. Derivation of shear strength expression

4.1. Strut and tie model

Concrete in between the diagonal cracks acts as an inclined strut, and the tension reinforcement acts as a tie. The strut and tie intersect at the node point. The arch action forms only after the diagonal crack, which facilitates in enhancing the shear strength. Moreover, due to arch action, the conventional sectional approaches are not applicable for deep beam design. The internal force transfer mechanism of a deep beam is shown in Figure 3.

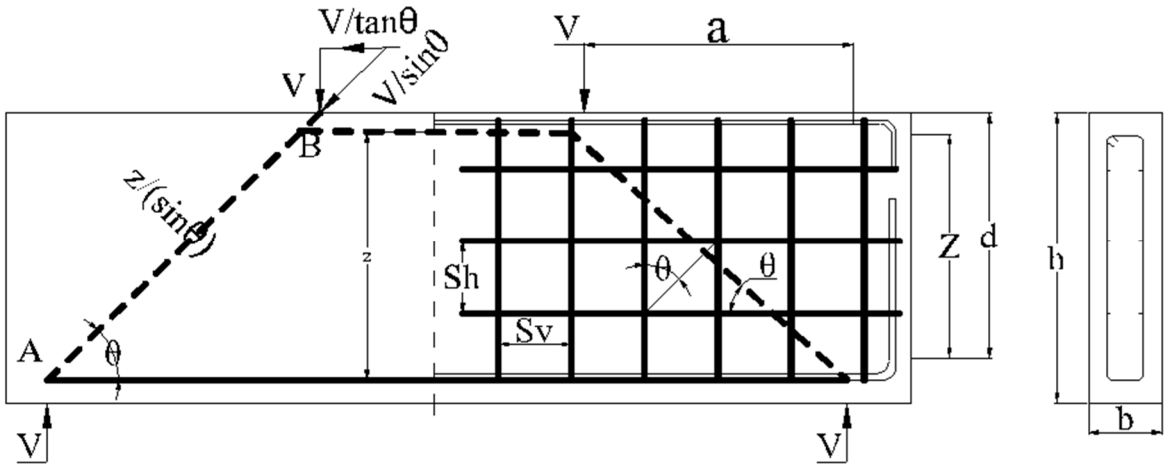

Figure 3. Strut-and-tie mechanism for RC deep beam.

Based on the strut-and-tie model approach, the force applied on the strut is $V/\sin\theta$. The internal forces resist the horizontal component of the strut force $V\cot\theta$. Furthermore, the inclination of the diagonal crack θ is idealized as $\tan^{-1}\left(\frac{0.8\,d}{a}\right)$. Using force equilibrium, the following formulation is arrived (Eq 1).

$$V\cot\theta = F\sin\theta \tag{1}$$

The total force F is the sum of contribution of concrete, horizontal and vertical web reinforcement, namely, F_C, F_H, and F_V as shown in Figure 4 (Eq 2).

$$V\cot\theta = \{F_c + F_H + F_v\}\sin\theta \tag{2}$$

In Figure 4 idealized diagonal splitting crack is shown in dashed lines.

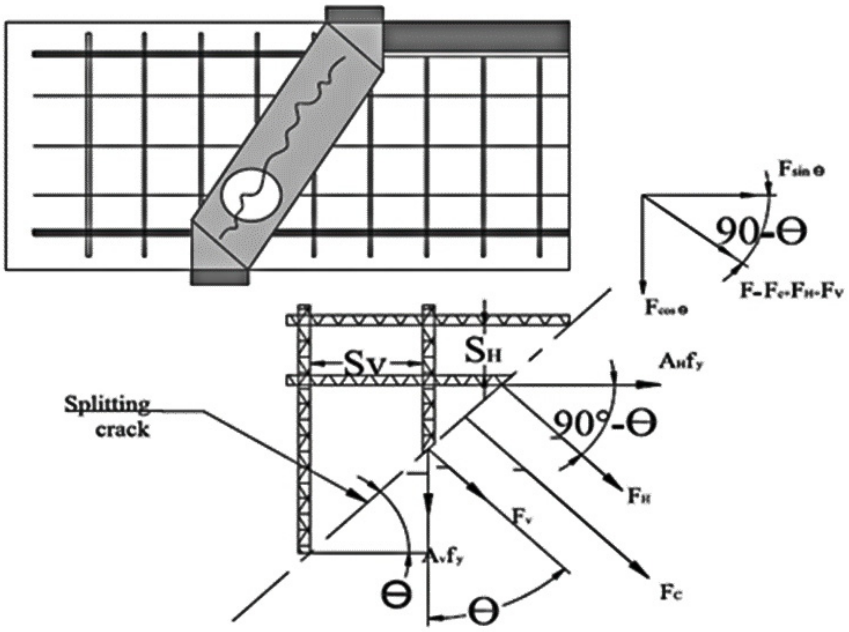

Figure 4. Internal forces resisting transverse tension.

4.2. Size-effect law

Bazant proposed size-effect law for beams made of brittle materials in the form of $f'_t = \frac{\mathrm{Bf_{ct}}}{\sqrt{1+\frac{\mathrm{d}}{\lambda \mathrm{d_a}}}}$ [16], and this size-effect equation is re-written as Eq3.

$$f'_t = \frac{Bf_{ct}}{\left(1+\frac{d}{\lambda d_a}\right)^{\alpha 1}} \tag{3}$$

where f'_t = nominal stress at failure, B and λ = empirical constants, f_{ct} = direct tensile strength of concrete, da = maximum size of aggregate, d = depth of the beam. Eurocode 2 expression for tensile strength of concrete $0.30\, f'^{\left(\frac{2}{3}\right)}_c$ is replaced by $\mathrm{A}f'^{\left(\frac{2}{3}\right)}_c$.

4.3. Effect of compressive strength of concrete

To overcome the compression softening effect, the concrete contribution is formulated by diagonal tension resistance rather than by axial compressive strength of the strut. The diagonal splitting crack is resisted by the tensile strength of concrete and the web reinforcement as shown in Figure 3. The contribution of concrete F_c acting normal to the diagonal (AB) can be determined from the equation given below (Eq 4).

$$F_c = \frac{f'_t bz}{\sin\theta} \tag{4}$$

where, lever arm $z = jd$ and $\left(\frac{bz}{\sin\theta}\right)$ is the area contributing for diagonal tensile strength. Rao and

Sundaresan derived a relation between lever arm and the percentage of tension reinforcement as $j = 0.62\rho^{-0.08}$ [17]. The expression is rewritten as $j = C\rho^{\alpha 2}$. By substituting f'_t and z, the following formulation has been proposed (Eq 5).

$$F_c = \frac{A f'^{\left(\frac{2}{3}\right)}_c b(C\rho^{\alpha 2} d)}{\sin\theta}\left(\frac{B}{\left(1+\frac{d}{\lambda d_a}\right)^{\alpha 1}}\right) \tag{5}$$

4.4. Web reinforcement mechanism

F_H and F_V are the internal force components perpendicular to the diagonal AB, which is offered by horizontal and vertical shear reinforcements. These force components are the multiples of total bars and tension force in each bar. Inclination and length of the idealized diagonal crack are given by "θ" and "$\frac{d}{\sin\theta}$", and the spacing of bars "*Sh*" and "*Sv*" are shown in Figures 5 and 6. The crack lengths are "d" and "$\frac{d}{\tan\theta}$" and these are multiplied by "$\frac{1}{x1S_h}$" and "$\frac{1}{y1S_v}$" for contribution to shear. Based on test data reported in the literature, the constants *x1* and *y1* have been approximately found to be 2.0.

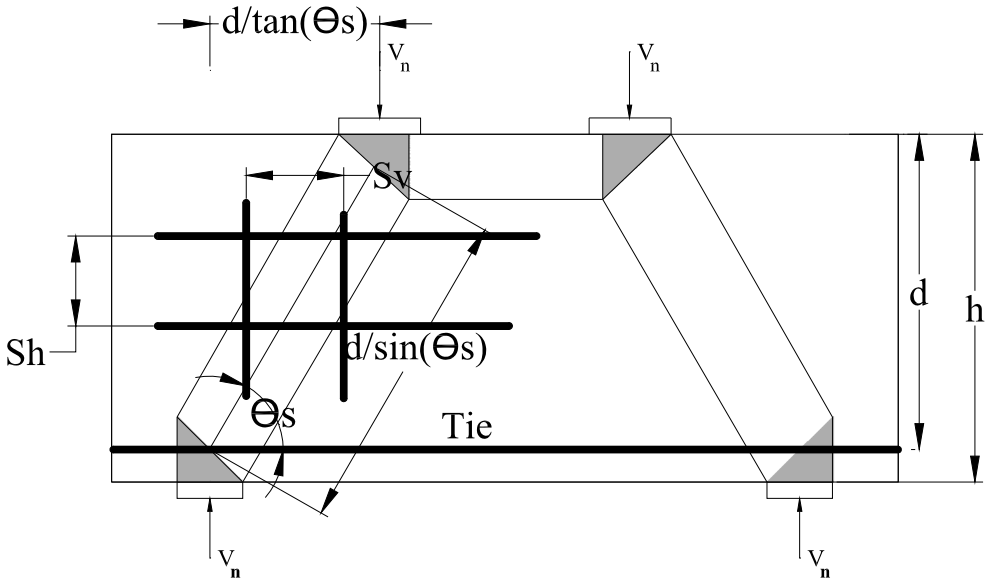

Figure 5. Web reinforcement mechanism.

In the above equations (Eqs 4 and 5), the number of horizontal and vertical bars is $n_h = \frac{d}{y1 \times s_h}$ and $n_v = \frac{d}{x1 \times s_v tan\,\theta}$. Thus, overestimation of web reinforcement is mitigated. Also, the effective shear span area is accounted for in the proposed equation (Eq 10).

To obtain the inclined force component, resistance offered by each horizontal and vertical bar is multiplied by $\sin\theta$ and $\cos\theta$ (Eqs 6 and 7).

$$F_H = n_h f_{yh} A_{sh} \sin\theta \tag{6}$$

$$F_V = n_v f_{yv} A_{sv} \cos\theta \tag{7}$$

The shear strength expression is obtained by incorporating the values of F_C, F_H and F_V.

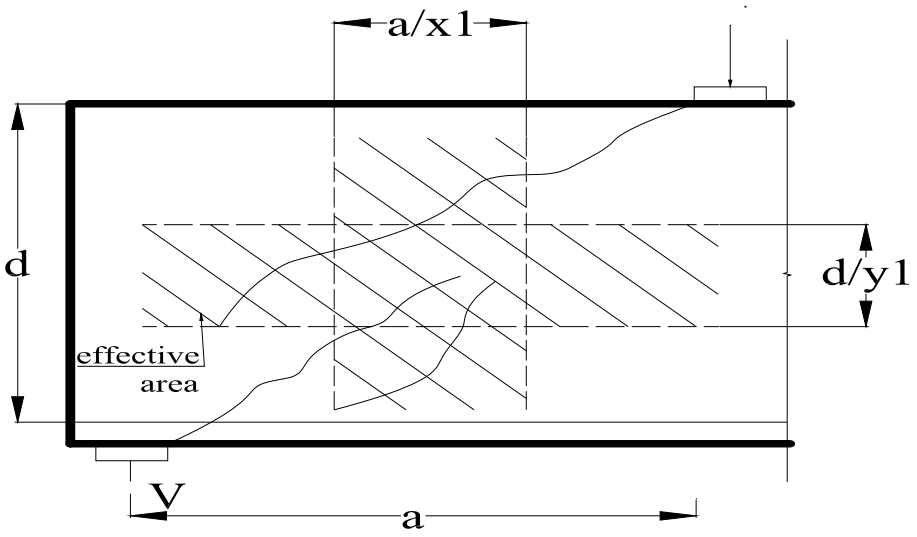

Figure 6. Effective area contributing shear resistance [18].

The contribution of web reinforcement and concrete are significantly dominated by a/d ratio. Thus, $\left(\frac{a}{0.8\,\mathrm{d}}\right)$ is substituted for $cot\,\theta$ in Eq 8. The constant D replaces the constants A, B and C.

$$V = \left\{ \frac{Df'^{\left(\frac{2}{3}\right)}_c \rho^{\alpha 2}}{cot\,\theta\,.\sin\theta} \sin\theta \left(\frac{1}{\left(1 + \frac{d}{\lambda d_a}\right)^{\alpha 1}} \right) bd + \frac{F_H \sin\theta + F_v \sin\theta}{cot\,\theta} \right\}$$

$$= \left\{ \frac{Df'^{\left(\frac{2}{3}\right)}_c \rho^{\alpha 2}}{\frac{a}{0.8\,d}} \left(\frac{1}{\left(1 + \frac{d}{\lambda d_a}\right)^{\alpha 1}} \right) bd \right. \tag{8}$$

$$\left. + \frac{0.5\, f_{yh} \rho_{sh} \sin\theta\,.\sin\theta + \frac{0.5 f_{yv} \rho_{sv} \cos\theta\,.\sin\theta}{tan\,\theta}}{\frac{a}{0.8\,d}} bd \right\}$$

4.5. Effect of shear span-depth ratio

The a/d ratio of the beams influences the shear strength, crack orientation, size dependence, web reinforcement and concrete contributions for the shear resistance. Effectively addressing the

influence of a/d ratio on the shear strength is a challenge. The term $\frac{D}{\left(\frac{a}{0.8\,d}\right)}$ is replaced by a consistent formulation $\frac{1}{log_{10}\left(1+\frac{a}{d}\right)}$. Thus, the generic form of the shear resistance is given in Eq 9.

$$V = \left\{ \begin{matrix} \frac{D\rho^{\alpha 2}}{log_{10}\left(1+\frac{a}{d}\right)} f'^{\left(\frac{2}{3}\right)}_{c} \left(\frac{1}{\left(1+\frac{d}{\lambda d_a}\right)^{\alpha 1}} \right) + \frac{0.5\, f_{yh}\rho_{sh}(sin\,\theta)^2}{\frac{a}{0.8d}} \\ +0.5\, f_{yv}\rho_{sv}\, cos\,\theta \times sin\,\theta \end{matrix} \right\} bd \tag{9}$$

In the Eq 9, various constants to be evaluated from the experimental data include *D*, *α1*, *α2* and *λ*.

4.6. Proposed shear strength equation

From the experimental data, using trial and error procedure, the constants *α1*, *α2* and *λ* are determined. Thus, a shear strength expression is formulated, which is given below (Eq 10).

$$V = \left\{ \frac{f'^{\left(\frac{2}{3}\right)}_{c}\, \rho^{\frac{1}{2}}}{log_{10}\left(1+\frac{a}{d}\right)} \left(\frac{1}{\left(1+\frac{d}{350 d_a}\right)^{0.75}} \right) + 0.4\frac{d}{a} f_{yh}\rho_{sh}(sin\,\theta)^2 + 0.25 f_{yv}\rho_{sv}\, sin\,2\theta \right\} bd \tag{10}$$

Limiting the design expression to V_{max} can give rise to conservative results. The limit is kept to resist cracking in concrete within service loads and to withstand against diagonal compression failure (Eq 11).

$$V_{max} = \left\{ \frac{7\, f'^{\left(\frac{1}{3}\right)}_{c}\, \rho^{\frac{1}{4}}}{log_{10}\left(1+\frac{a}{d}\right)} \right\} bd^{4/3} \tag{11}$$

The various power coefficients in the expression for Vmax are arrived at by plotting Vu/bd versus *d*, *f'c*, $log_{10}\left(1+\frac{a}{d}\right)$ and ρ. The determined power coefficients are $f'^{\left(\frac{1}{3}\right)}_{c}$, $\rho^{\frac{1}{4}}$, $log_{10}\left(1+\frac{a}{d}\right)^{-1}$ and $d^{4/3}$. The above coefficients are adjusted so that the strength ratios (VnTEST/VnPRO) fall in the range of 1.0 to 2.0.

5. Finite element analysis

Using the ABAQUS program along with codal provisions of ACI 318-14, a statistical study was done to know the shear strength of deep beams. CDP model was used to know its behavior. Figures 7 and 8 represents the concrete compression behavior and tension behavior for concrete. Figure 9 represents the stress strain relationship for reinforcement in ABAQUS model.

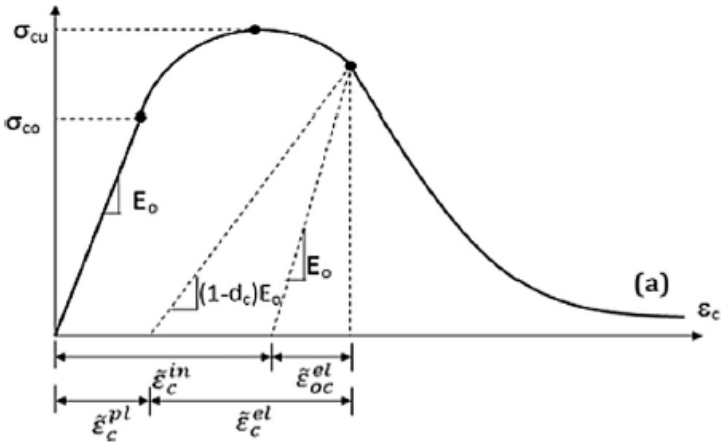

Figure 7. Concrete compression behavior in ABAQUS Software.

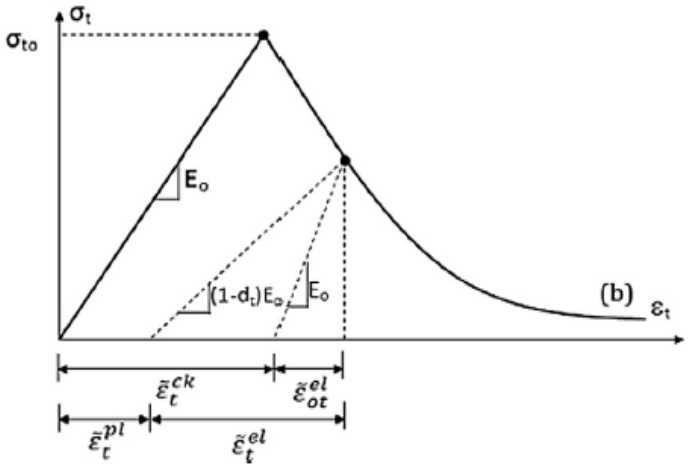

Figure 8. Tension behavior for concrete based on stress strain relationship in ABAQUS.

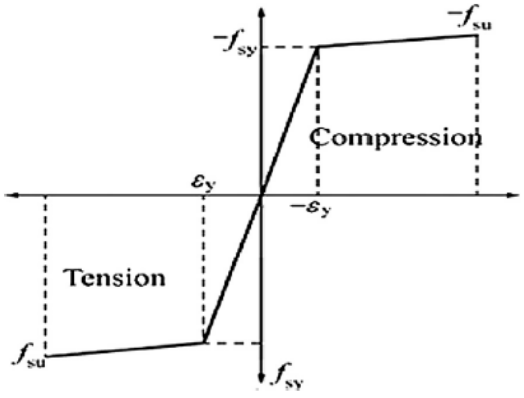

Figure 9. Stress strain relationship for reinforcement in FE model.

Table 4 gives the values of young's modulus, Poisson's ratio, dilation angle, eccentricity for the analysis of deep beams using solid 65 model type in Abaqus.

Table 4. Modal parameters for deep beams in Abaqus.

S. No	Modal parameter	Value
1	Youngs modulus (Mpa)	29580.4
2	Poisson's ratio	0.2
3	Dilation angle (ψ)	31
4	Eccentricity (e)	0.1
5	Second stress invariant (K)	0.67
6	σbo/σco	1.16

K = ratio of second stress invariant on tensile meridian to compressive meridian; σbo/σco = ratio of initial equibiaxial compressive yield stress to initial uniaxial compressive yield stress.

6. Results and discussions

6.1. Existing shear strength expressions

The shear strength of beams has been evaluated using the following codes: IS 456-2000 [19], ACI 318-14 [20] strut-and-tie provision. In addition to that shear strength of beams is evaluated using the expressions suggested by Zsutty, Tang et al., Russo et al. [21–23]. Aforesaid equations are briefly named as Zsutty, Tang, Russo whereas the shear force calculated using these equations are V_n^{ZUTTY}, V_n^{TANG}, V_n^{RUSSO}. Table 5 represents the existing shear strength expressions by various codes and researchers.

Table 5. Existing shear strength expressions.

Modals	Shear strength expression
Zutty [21]	$V_n^{ZUTTY} = \left(\left(2.5\frac{d}{a}\right)2.2\left(f'_c\rho\frac{d}{a}\right)^{1/3} + \rho_v f_{yv}\right)bd; for\ a/d \le 2.5$
IS 456 [19]	$V_n^{IS\,456} = f_y A_{st} z$; where z = $\begin{cases} 0.2(l+2D)\ when\ 1 \le \frac{l}{D} \le 2 \\ 0.6\ l\ when\ \frac{l}{D} < 1 \end{cases}$
Tang et al. [22]	$A_{str} = b_w(l_a \cos\theta_s + l_b \sin\theta_s);\ A_{ct} = b_w z_s / \sin\theta_s$
	$z_s = h - \frac{l_a}{2} - \frac{l_c}{2};\ \tan\theta_s = \frac{h-\frac{l_a}{2}-\frac{l_c}{2}}{a}$
	$V_{ds} = \frac{f_{ct}A_{ct} + f_{yw}A_w \sin(\theta_w+\theta_s) + 2f_y A_s \sin\theta_s}{2\cos\theta_s}$
	$V_{dc} = f'_c A_{str} \sin\theta_s$
	$\frac{1}{V_n^{TANG}} = \frac{1}{V_{ds}} + \frac{1}{V_{dc}}$

Continued on next page

Modals	Shear strength expression
Russo et al. [23]	$V_n^{RUSSO} = 0.545\left(k\chi f_c' \cos\theta + 0.25\rho_h f_{yh}\cot\theta + 0.35\frac{a}{d}\rho_v f_{yv}\right)$bd $\chi = \left[0.74\left(\frac{f_c'}{105}\right)^3 - 1.28\left(\frac{f_c'}{105}\right)^2 + 0.22\left(\frac{f_c'}{105}\right) + 0.87\right]$
ACI 318-14 [20], Strut-and-tie provision	$V_{A1} = 0.80 \times 0.85 f_c'\, l_p b$ $V_{B1} = 0.85 f_c'\, l_p b$ $V_{AD} = A_s f_{ys} \tan\theta$ $V_{A2} = 0.80 \cdot 0.85 f_c'\, w_t b \tan\theta$ $V_{B2} = 0.85 f_c'\, d_a b \tan\theta$ $V_{A3} = 0.80 \cdot 0.85 f_c'\, \sin\theta\, b(l_p \sin\theta + w_t \cos\theta)$ $V_{B3} = 0.85 f_c'\, \sin\theta\, b(l_b \sin\theta + d_a \cos\theta)$ $V_n^{ACI\ 318-STM} = min[V_{A1}; V_{B1}; V_{AD}; V_{A2}; V_{B2}; V_{A3}; V_{B3}]$
Proposed equation	$V_n^{PRO} = \left\{\frac{D\rho^{\alpha 2}}{log_{10}\left(1+\frac{a}{d}\right)} f_c'^{\left(\frac{2}{3}\right)}\left(\frac{1}{\left(1+\frac{d}{\lambda d_a}\right)^{\alpha 1}}\right) + \frac{0.5\, f_{yh}\rho_{sh}(\sin\theta)^2}{\frac{a}{0.8\, d}} + 0.5\, f_{yv}\rho_{sv}\cos\theta\,.\sin\theta\right\} bd$

6.2. Comparison of predicted equation with existing shear strength equations

6.2.1. Effect of depth on shear strength

Zsutty [21] equation and proposed equation predict for small, medium and large size beams uniformly. At the same time, for the deep beams with depth nearly 1800 mm, strut-and-tie models such as Tang [22], ACI-STM [20] predicts in the range of 25% to 60 % of the ultimate strength. Hence, Tang [22] and ACI-STM [20] models are over conservative for the large size beams.

6.2.2. Effect of compressive strength of concrete

By introducing the strength reduction factor in ACI 318-14, most of the strength ratios $\frac{V_n^{TEST}}{V_n^{PRE}}$ of high strength concrete beams are higher than 1.0. Also, it is noted that ACI 318-08 VnMax scatters equally above and below the safety line. Thus, mean of shear strength ratio of ACI 318-08 VnMax is equal to 1.00. In order to improve the conservativeness, ACI 318-14 introduced the strength reduction factor in maximum design shear force (0.75), which gives reasonable amount of conservativeness.

6.2.3. Effect of tension reinforcement

Zsutty [21] equation and proposed equation predicted the beams provided with low and a high

percentage of tension reinforcement uniformly. As the percentage of tension reinforcement increases, strength ratios increase in Tang [22], ACI-STM [20]. Beams with a low percentage of tension reinforcement exhibit flexure as well as shear crack. Empirical equations such as ACI 318-14 VnMax are derived only from the shear test results. Due to this reason, these equations overestimate some beams with a low percentage of tension reinforcement. While comparing direct strut-and-tie models with the proposed equation, effect of percentage of tension reinforcement on shear strength is accounted for properly.

6.2.4. Effect of vertical web reinforcement

Zsutty [21] equation did not address the influence of vertical web reinforcement effectively. At the same time, the proposed equation predicts very close to the strength ratio line 1.0. As usual, Russo [23] equation predicted the beams with low and high quantity of vertical web reinforcement uniformly. Other strut and tie models Tang [22] and ACI-STM [20] show reasonable scatter. While comparing the proposed equation with all other equations, it is clear that almost all the beams are underestimated.

6.3. Validation of results

The ratio of the predicted shear strength-to-experimentally observed shear strength is defined as the strength ratio. Among all the predictions, mean of the strength ratios according to ACI-STM [20] and proposed equation are close to the safety line 1.0, where the proposed equation has a mean value of 0.94 and 1.26 according to ACI-STM [20]. Moreover, the mean of the strength ratio according to IS 456 [19] has been observed to be the lowest (0.448). The mean values of Zsutty [21] and Tang [22] equations are 0.84.

The standard deviation (SD) of IS 456 strength ratio is the least among all the predictions according to all the standards. Subsequently, equations such as the proposed equation, ACI 318-STM [19] and Zsutty [21] showed a 12 % deviation from the mean.

Though ACI 318-14 equation showed very close average value to the safety line, it exhibits the highest coefficient of variation (COV) (2.4%) than all other predictions. Conversely, IS 456 [19] equation predicts the strength ratio with least COV of 0.4%. Equations such as Zsutty [21], Tang [22], Russo [23–25], and proposed equation showed almost same COV. From the above analysis, it is observed that irrespective of the size, the proposed equation gives uniform prediction with mean 0.94 and standard deviation 0.14. Since the Indian standard does not consider the effect of size, compressive strength and web reinforcement, strength of all the beams were overestimated. Evaluation of ACI 318-14 [20] strength reduction factor using the experimental results is discussed in the following section.

6.4. Evaluation of strength reduction factor

Table 6 shows the strength reduction factor of ACI 318-14 [19] expression for maximum design shear strength of RC deep beams has been evaluated. Strength ratios of ACI 318-14 [19] $\frac{{v_n}^{ACI318-14}}{{v_n}^{TEST}}$

is given in Table 6. For all the beams, the ratio $\frac{v_n{}^{ACI318-14}}{v_n{}^{TEST}}$ is greater than 1.0. Thus, strength reduction factor is adequate to consider the shear compression mode of failure. The mean value of ACI 318-14 [20] of strength ratio is 1.26 and standard deviation is 0.15. From the above analysis, it can be concluded that the strength reduction factor is effective when the beams failed in shear compression.

Table 6. Shear strength predictions.

S. No	Beam ID	$\frac{v_n{}^{ACI\,318-14}}{v_n{}^{TEST}}$	$\frac{v_n{}^{is\,456}}{v_n{}^{TEST}}$	$\frac{v_n{}^{ZUTTY}}{v_n{}^{TEST}}$	$\frac{v_n{}^{TANG}}{v_n{}^{TEST}}$	$\frac{v_n{}^{RUSSO}}{v_n{}^{TEST}}$	$\frac{v_n{}^{PRE}}{v_n{}^{TEST}}$
1	1D500	1.33	0.46	0.88	0.87	0.79	0.98
2	2D500	1.33	0.46	0.88	0.84	0.79	0.98
3	3D500	1.19	0.41	0.79	0.75	0.70	0.85
4	4D500	1.04	0.36	0.69	0.66	0.60	0.72
5	5D500	1.22	0.45	0.83	0.88	0.76	1.00
6	6D500	1.50	0.55	1.02	1.08	0.90	1.14
MEAN		1.26	0.448	0.84	0.84	0.75	0.94
SD		0.156	0.06	0.1	0.14	0.1	0.14
COV		0.024	0.004	0.01	0.02	0.01	0.02

6.5. Comparison between experimental and FE modal results

Table 7 gives the comparison of ultimate loads between analytical and experimental results. From Figure 10, it can be seen that FE model gave high prediction of ultimate loads for deep beams. An average of 96.3% was observed between the experimental and FE model results and thus FE model shows a good efficiency in simulating the deep beams.

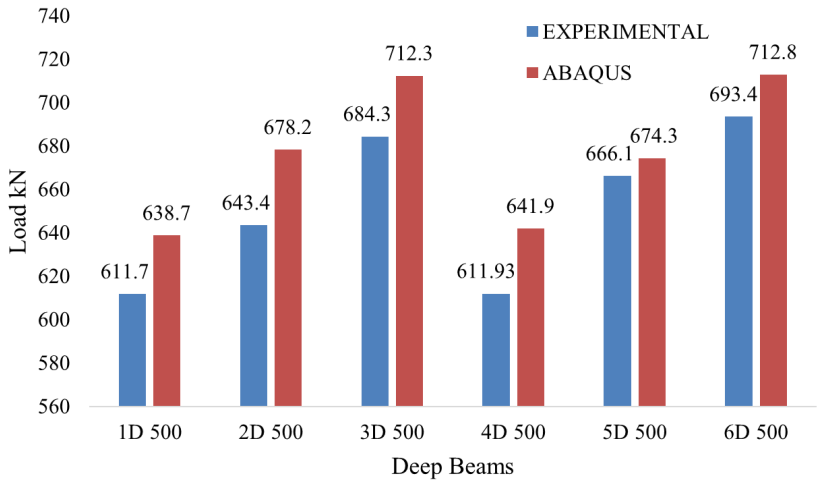

Figure 10. Comparison of ultimate loads of all deep beam specimens.

Table 7. Comparison of ultimate loads between analytical and experimental results.

S. No	Specimen	Pu Exp (kN)	Pu Abaqus (kN)	Pu Exp/Pu Abaqus (%)
1	1D500	611.7	638.7	95.77
2	2D500	643.4	678.2	94.87
3	3D500	684.3	712.3	96.07
4	4D500	611.93	641.9	95.33
5	5D500	666.1	674.3	98.78
6	6D500	693.4	712.8	97.28

Table 8 gives the comparison of ultimate deflection between analytical and experimental results. It can be seen that experimental results gave high prediction of deflection values in comparison with FE model for all the deep beams. An average of 107.8% was observed between these two and FE model gave slightly less prediction in terms of deflection.

Table 8. Comparison of ultimate deflection between analytical and experimental results.

S. No	Specimen	Pu Exp (mm)	Pu Abaqus (mm)	Pu Exp/Pu Abaqus (%)
1	1D500	5.47	5.14	106.42
2	2D500	6.12	5.86	104.44
3	3D500	6.82	6.14	111.07
4	4D500	6.46	6.08	106.25
5	5D500	6.43	5.91	108.80
6	6D500	6.62	6.02	109.97

6.6. Load–deflection behavior

To verify the proposed equation, a comparison is done with the load and deflection behavior Figure 11 gives the experimental and analytical comparison of load vs deflection of all deep beam specimens. A close correlation between Fe model predicted results and experimental results have been found. Deep beams 5D 500 and 6D 500 are in close agreement and almost they are similar. In the remaining deep beams, the FE model results have over predicted.

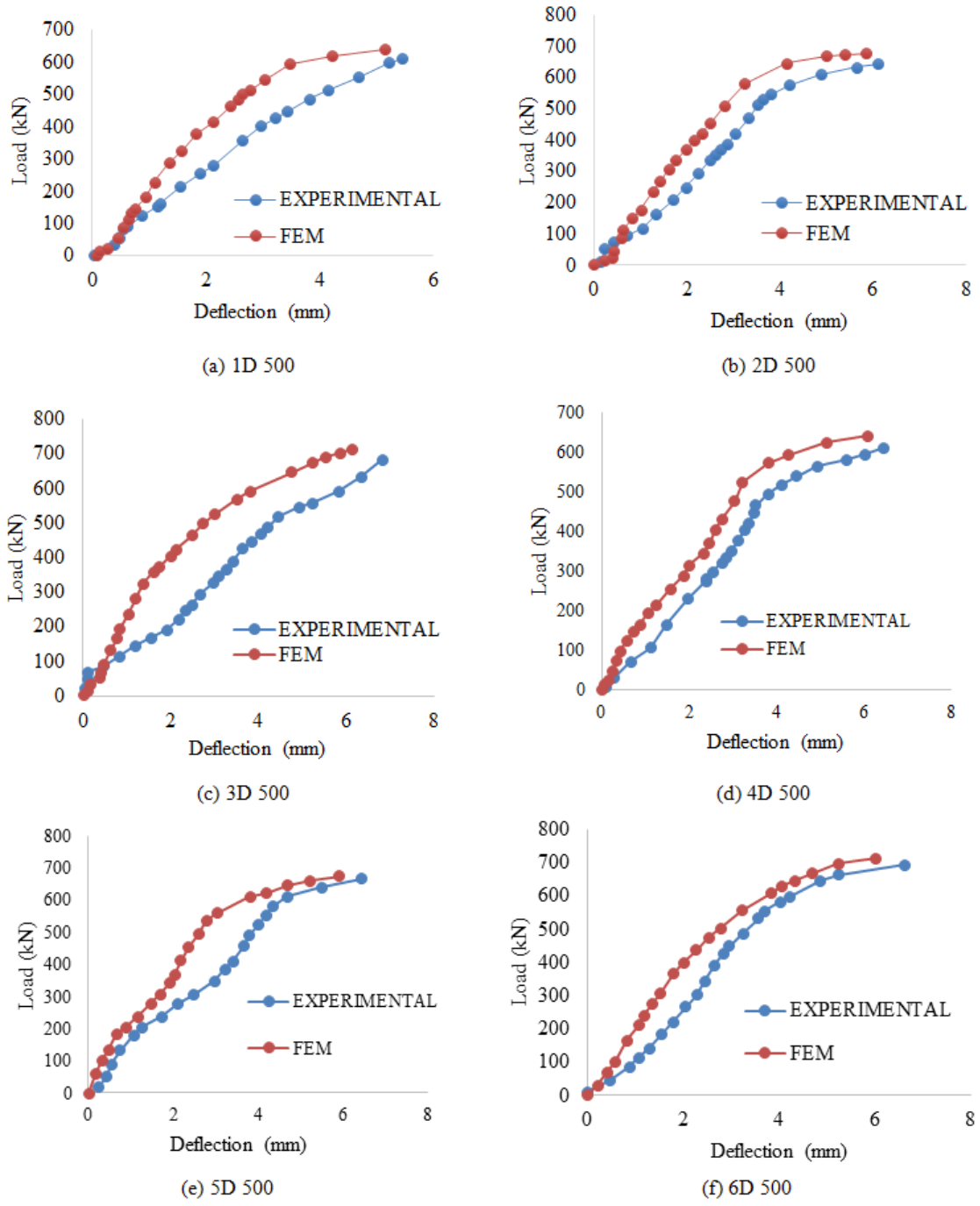

Figure 11. Experimental and analytical comparison of load vs deflection of deep beam specimens.

6.7. Damage Tension in FE model

Three dimensional isoparametric solid elements (SOLID65) were used in the FE model. Figure 12 shows the tensile crack patterns due to tensile stress of the FE model (DAMAGET). The tension cracks started from the position of support and reached to the point of application of load at an average angle of 38°. In the deep beam 3D 500, the maximum tension is found near the top left

1/3rd portion whereas in the deep beam 2D 500 and 6D 500, the maximum tension is found near the top right 1/3rd position. Flexural cracks were also obtained in both experimental and FE model in all the deep beams.

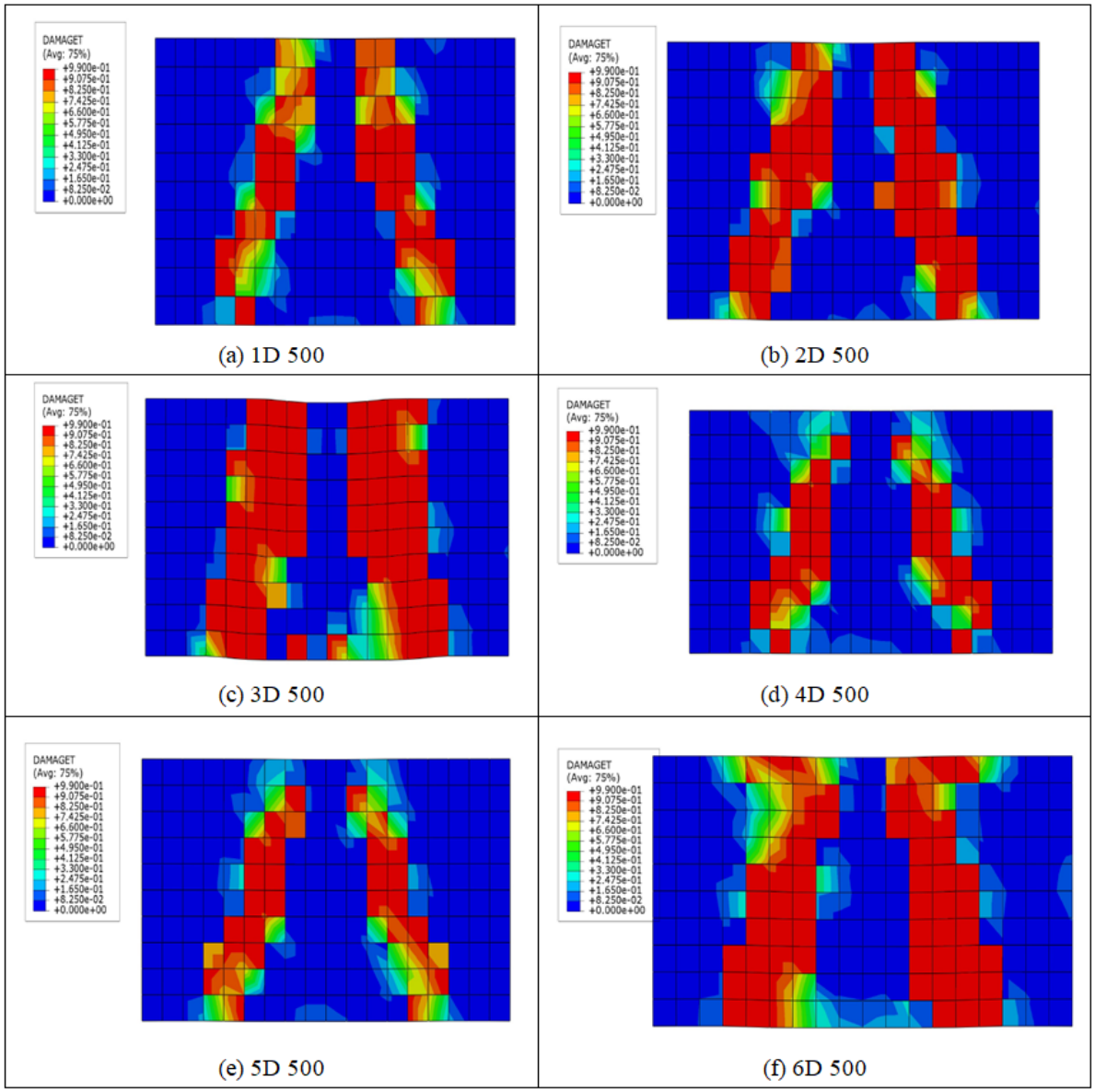

Figure 12. Crack pattern of FE damaged tension model.

6.8. Strain distribution

The strain distribution is considered very important to know about the tied arch mechanism and its formation in the specimens. Figure 13 gives the strain distribution at the bottom layer of the beam 6D 500 as the load is increasing from 0 to ultimate load. The strain readings increased rapidly at the first crack in the mid span. Since more cracks appeared near the supports, measured strains also increased near the supports whereas in the uncracked region, the strain readings showed minimal strain changes.

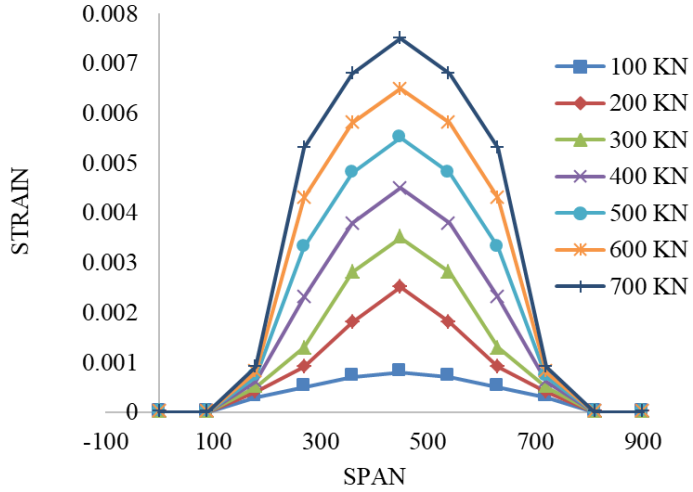

Figure 13. Strain distribution along the bottom layer in beam 6D 500 as the load is increasing.

7. Conclusions

Six reinforced concrete deep beams were analyzed numerically and compared with experimental results and these were analyzed to study the parameters like size effect, compressive strength effect, web reinforcement mechanism, shear span-depth ratio, load deflection behavior, tension damage and strain distribution and the following conclusions were drawn.

a. The proposed shear strength equation predicts 80% of the experimental data in the range of 66–110% of measured shear strength, whereas other design procedures are over either conservative, which is uneconomical, or overestimating, which is unsafe.
b. Moreover, the proposed equation is validated with the experimental results.
c. The predicted shear strength is compared with the experimental shear strength. The calculated nominal shear stress γ_n^{PRE} versus the measured shear stress γ_n^{TEST} is compared.
d. It has been observed that prediction by design equations and experimental shear strength are in close relation with each other.
e. Although ACI 318-08 maximum shear force equation gives a mean value of 1.08, a strength reduction factor is introduced in ACI 318-14. It shows the importance of analysis based on the percentage of overestimation. But in general, STM code equations give conservative results.
f. A variation of 8% has been found between experimental and FE model results in terms of displacement whereas a variation of 22% has been found in terms of ultimate loads.
g. The stress contours suggested high stresses in the path of cracks and low stresses in the uncracked regions.

Acknowledgments

I would like to acknowledge Dr. P. Poluraju and Dr. C. Khed Veerendra Kumar my research guide for helping in investigating the behavior of deep beams. I am grateful to Koneru Lakshmaiah Education Foundation (KL Deemed to be university) for their continuous support and assistance.

Conflict of interest

All authors declare no conflicts of interest in this paper

References

1. Harsha GS, Vidyadhari S (2018) Effect of shear reinforcement on the structural behaviour of the reinforced concrete deep beam. *Int J Eng Technol* 7: 189–192.
2. Pavani K, Harsha GS (2018) Analytical and experimental study on composite deep beams with rolled section reinforcement. *Int J Eng Technol* 7: 7–11.
3. Tasleema M, Kumar MA, Raj JL (2019) Evaluation of shear strength of deep beams using artificial neural networks. *International Conference on Advances in Civil Engineering (ICACE-2019)*, 7: 341–345.
4. Shyam Prakash K, Rao CH (2016) Study on compressive strength of quarry dust as fine aggregate in concrete. *Adv Civ Eng* 2016: 1–5.
5. Veerendrakumar CK, Bashar SM, Liew MS, et al. (2020) Development of response surface models for self-compacting hybrid fibre reinforced rubberized cementitious composite. *Const Build Mat* 232: 1–19.
6. Sravanthi D, Kumar YH, Kumar BSC (2020) Experimental study on reinforced geopolymer concrete deep beams. *IOP Conf Ser Mater Sci Eng* In press.
7. Kumar BSC, Karuppusamy S, Ramesh K (2019) Correlation between compressive strength and split tensile strength of GGBS and MK based geopolymer concrete using regression analysis. *J Mech Cont Math Sci* 14: 21–36.
8. Kumar BSC, Ramesh K (2018) Analytical study on flexural behaviour of reinforced geopolymer concrete beams by ANSYS. *IOP Conf Ser Mater Sci Eng* 455: 012065.
9. Deepthi K, Chaitanya JD and Rangarao MLS (2019) Experimental investigation of shear behavior in flexure members. *Int J Recent Techno Eng* 7: 305–310.
10. Kumar KH, Poluraju P (2017) Comparative study on flexural behavior of lightweight aggregate RC beams. *Intl J Civil Eng Tech* 8: 1546–1561.
11. Srudhira B, Kumar MA, Chari KJB (2019) Evaluation of shear behaviour of RC beams using CFRP. *Int J Recent Techno Eng* 7: 329–333.
12. ABAQUS CAE (2007) ABAQUS Inc. Available from: http://130.149.89.49:2080/v2016/index.html.
13. ACI 318 (2008) Building code requirements for structural concrete and commentary. Available from: https://www.concrete.org/chapters/getchapterdocument.aspx?DocID=53344.
14. Ibrahim MM (2017) Three-dimensional nonlinear finite element analysis of concrete deep beam reinforced with GFRP bars. *HBRC J* 13: 25–38.
15. Ibrahim MA, Thakeb A, Mostfa AA et.al (2018) Proposed formula for design of deep beams with shear openings. *HBRC J* 14: 450–465.
16. Bazant ZP, Kazemi TM (1991) Size effect on diagonal shear failure of beams without stirrups. *ACI Struct J* 88: 268–276.
17. Rao GA, Sundaresan R (2014) Size dependent shear strength of reinforced concrete deep beams based on refined strut-and-tie model. *J Front Constr Eng* 3: 9–19.
18. Kuok H, Matamoros A (2003) Design of simply supported deep beams using strut-and-tie models. *ACI Struct J* 100: 704–712.

19. IS 456. Indian standard plain and reinforced concrete code of practice. Bureau of Indian Standards, 2000. Available from: https://elibrarywcl.files.wordpress.com/2015/02/plain-and-reinforced-concrete.pdf.
20. ACI 318. Building code requirements for structural concrete. ACI Committee, 2014. Aailable from: https://www.concrete.org/Portals/0/Files/PDF/Previews/318-14_preview1.pdf.
21. Zsutty T (1968) Beam shear strength prediction by analysis of existing data. *ACI J Proc* 65: 943–951.
22. Tang CY, Tan KH (2004) Interactive mechanical model for shear strength of deep beams. *J Struct Eng-Asce* 130: 1534–1544.
23. Russo G, Veni R, Pauletta M (2005) Reinforced concrete deep beams-shear strength model and design formula. *ACI Struct J* 102: 429–437.
24. Harsha GS, Poluraju P (2019) Shear strength of deep beams: a state of art. *International Conference on Advances in Civil Engineering (ICACE-2019)*, 7: 532–535.
25. Harsha GS, Poluraju P (2021) Modified strut & tie method and truss reinforcement for shear strengthening of reinforced concrete deep beams. *Int J Tech* 12: 65–77.

AIMS Press